Human Molecular Genetics, 1998, Vol. 7, No. 12 **1841–1849**

ARTICLE

Goosecoid-like (*Gscl*), a candidate gene for velocardiofacial syndrome, is not essential for normal mouse development

Bruno Saint-Jore, Anne Puech, Jörg Heyer[1], Qingcong Lin, Cedric Raine[2], Raju Kucherlapati[1] and Arthur I. Skoultchi*

Department of Cell Biology, [1]Department of Molecular Genetics and [2]Department of Pathology, Albert Einstein College of Medicine, 1300 Morris Park Avenue, Bronx, NY 10461, USA

Received July 15, 1998; Revised and Accepted August 28, 1998

Velocardiofacial syndrome (VCFS) and DiGeorge syndrome (DGS) are characterized by a wide spectrum of abnormalities, including conotruncal heart defects, velopharyngeal insufficiency, craniofacial anomalies and learning disabilities. In addition, numerous other clinical features have been described, including frequent psychiatric illness. Hemizygosity for a 1.5–3 Mb region of chromosome 22q11 has been detected in >80% of VCFS/DGS patients. It is thought that a developmental field defect is responsible for many of the abnormalities seen in these patients and that the defect occurs due to reduced levels of a gene product active in early embryonic development. *Goosecoid-like* (*GSCL*) is a homeobox gene which is present in the VCFS/DGS commonly deleted region. The mouse homolog, *Gscl*, is expressed in mouse embryos as early as E8.5. *Gscl* is related to *Goosecoid* (*Gsc*), a gene required for proper craniofacial development in mice. *GSCL* has been considered an excellent candidate for contributing to the developmental defects in VCFS/DGS patients. To investigate the role of *Goosecoid-like* in VCFS/DGS etiology, we disrupted the *Gscl* gene in mouse embryonic stem cells and produced mice that transmit the disrupted allele. Mice that are homozygous for the disrupted allele appear to be normal and they do not exhibit any of the anatomical abnormalities seen in VCFS/DGS patients. RNA *in situ* hybridization to mouse embryo sections revealed that *Gscl* is expressed at E8.5 in the rostral region of the foregut and at E11.5 and E12.5 in the developing brain, in the pons region and in the choroid plexus of the fourth ventricle. Although the gene inactivation experiments indicate that haploinsufficiency for *GSCL* is unlikely to be the sole cause of the developmental field defect thought to be responsible for many of the abnormalities in VCFS/DGS patients, its localized expression during development could suggest that hemizygosity for *GSCL*, in combination with hemizygosity for other genes in 22q11, contributes to some of the developmental defects as well as the behavioral anomalies seen in these patients. The mice generated in this study should help in evaluating these possibilities.

INTRODUCTION

Interstitial deletions within human chromosome 22q11 are associated with two related autosomal dominant genetic disorders, velocardiofacial syndrome (VCFS; MIM 19263) and DiGeorge syndrome (DGS; MIM 188400) (1,2). The two syndromes are quite common, with a prevalence estimated to be 1 in 4000 live births (3). The typical phenotypic features of VCFS include cleft palate, velopharyngeal insufficiency resulting in hypernasal speech, conotruncal cardiac anomalies, a characteristic facial dysmorphology and learning disabilities (4,5). The penetrance and severity of each anomaly vary significantly among VCFS patients and numerous additional anomalies have also been described, including skeletal muscle hypotonia, thrombocytopenia, mental retardation and psychiatric illness (6–8). DGS patients share many of the features seen in VCFS patients, including hypocalcemia due to hypoparathyroidism and immune deficiencies due to congenital hypoplasia or aplasia of the thymus (5).

Most of VCFS/DGS patients have similar, large hemizygous deletions in 22q11 (9–12). Some patients have unique 22q11 deletions or translocations and the description of such patients has led to various hypotheses concerning the definition of a critical region in which the gene or genes responsible for these

*To whom correspondence should be addressed. Tel: +1 718 430 2169; Fax: +1 718 430 8574; Email: skoultch@aecom.yu.edu

syndromes is expected to reside (13,14). However, there is no consensus regarding the definition of the critical region and attempts to narrowly define such a region based on the positions of chromosomal rearrangements are suspect because of the possibility that genomic rearrangements may exert position effects on expression of distant genes (15–18). At least 18 genes and several ESTs have been identified within the VCFS/DGS commonly deleted region, but to date no mutations in these genes have been reported in patients that lack any detectable deletion or rearrangement in 22q11. An alternative approach to identifying patients with mutations in a specific gene(s) is to evaluate the possible contribution of genes in 22q11 to the syndromes by analyzing animals in which expression of a candidate gene has been inactivated. The development of methods for introducing gene-specific inactivating mutations into the germline of mice provides such an opportunity.

A substantial body of evidence points to a defect in early embryonic development as the cause of many of the abnormalities present in VCFS/DGS patients. Several of the tissues and organ systems that are affected in these syndromes are derived from the pharyngeal arches and pouches. During early development these structures are populated by migrating cephalic neural crest cells. The importance of cephalic neural crest-derived cells in the development of the conotruncal region of the heart, the thymus and parathyroid glands and the connective tissues of the lower face and neck, all structures that are affected in VCFS/DGS, has been demonstrated by microablation and transplantation studies in avian embryos (reviewed in refs 19–21). Based on these observations it is reasonable to hypothesize that a gene or genes located within the 22q11 commonly deleted region is involved in the processes of neural crest cell migration or differentiation in the pharyngeal arches and that haploinsufficiency of such a gene(s) disrupts proper development of these systems leading to multiple organ and tissue abnormalities. Therefore, an important criterion for the involvement of a candidate gene in VCFS/DGS etiology is that it be expressed in the developing embryo when these processes occur. Alternatively, or in addition, haploinsufficiency of individual genes may contribute to specific aspects of the VCFS/DGS phenotype by causing a reduction in the amount of gene products required for proper organogenesis of specific tissues at later stages of development.

Homeodomain-containing proteins represent a very large family of transcription factors that play key roles in many developmental processes (22–25). Studies of mice in which specific members of this family have been inactivated indicate that several of them are involved in developmental processes relevant to VCFS/DGS etiology (26–29). However, the human orthologs of these genes are not located within human chromosome 22q11. Our group and others recently described a gene, *Goosecoid-like* (*GSCL*), lying in 22q11, that is capable of encoding a homeodomain-containing protein (30,31). *GSCL* is related to a previously described homeobox gene, *Goosecoid* (*GSC*) (32), in both genomic organization and the sequence of the homeodomain. *Gsc* is expressed in developing mouse embryos (33,34) and gene inactivation experiments show that it is required for proper craniofacial and rib cage development (27,28,35). We found that *Gscl* is also expressed in early mouse embryos, from E8.5 to 10.5, the time of neural crest migration and differentiation in the pharyngeal arches, as well as a later times during organogenesis (30). Thus, *Gscl* would appear to be an excellent candidate for contributing to VCFS/DGS etiology. To investigate this possibility we disrupted the *Gscl* gene in mouse embryonic stem cells and produced mice homozygous for the disrupted allele. These mice are viable and do not exhibit any of the major anatomical abnormalities seen in VCFS/DGS patients. Nevertheless, the sites of *Gscl* expression during mouse embryogenesis suggest that hemizygosity for *GSCL*, in combination with hemizygosity for other genes in 22q11, could contribute to some aspects of the VCFS/DGS phenotype.

RESULTS

Generation of ES cells with a disrupted *Gscl* gene

The mouse *Gscl* gene contains an open reading frame of 618 bp encompassed in three exons that span 1293 bp of genomic DNA sequence (36). To disrupt the *Gscl* gene a targeting vector (Fig. 1) was constructed in which a 2.3 kb segment including the complete open reading frame, 840 bp of the putative promoter region and 100 bp 3′ of the termination codon (36) was deleted and replaced by a cassette containing a gene that confers resistance to hygromycin. The cassette also included two other features that are useful for future genomic manipulations: a LoxP site and a promoterless gene that can confer resistance to puromycin. The linearized targeting vector was electroporated into WW6 ES cells (37) and cells resistant to hygromycin were selected. Genomic DNA from 384 hygromycin-resistant clones were pooled (6 colonies/pool) and tested for gene targeting events by long-range PCR utilizing a primer lying outside the targeting construct (*Gscl* K03, Fig. 1) and a primer lying in the hygromycin resistance gene (Hyg-K01, Fig. 1). Twenty one pools gave the expected 5.6 kb PCR product and upon subsequent analysis a total of 31 colonies exhibited the 5.6 kb product (Fig. 2). The results correspond to an overall targeting frequency of 8.1% among the hygromycin-resistant clones.

Production of *Gscl* null mice

Several ES cell clones (Fig. 2) containing the modified *Gscl* locus were injected into C57BL/6 blastocysts to generate chimeric mice. Two cell lines generated chimeras ranging in chimerism between 50 and 90% as judged by coat color. Male chimeras were mated with C57BL/6 females. PCR analysis of tail DNA from offspring carrying the dominant, ES cell-derived agouti coat color marker showed that the chimeras could transmit the modified *Gscl* allele (data not shown). To determine whether *Gscl* is necessary for mouse development, mice heterozygous for the modified *Gscl* allele were interbred. Examples of Southern blot analyses of tail DNA from the progeny (Fig. 3A) indicate that animals homozygous for the modified *Gscl* allele are viable. Of 239 animals examined in this way, 64 (26.8%) carried only the wild-type allele, 121 (50.6%) carried one copy of the modified allele and 54 (22.6%) carried two copies of the modified allele. The ratio of the three classes of animals is not significantly different from the expected values for Mendelian transmission of the two alleles.

To show that the *Gscl* gene is indeed a single copy gene, Southern blots of tail DNA were probed with a segment of *Gscl* exon 1 that was deleted in the targeting vector. No hybridizing bands were observed in DNA samples from mice homozygous for the modified allele (Fig. 3B). Since the modified *Gscl* locus is expected to be deleted of the three *Gscl* exons as well as

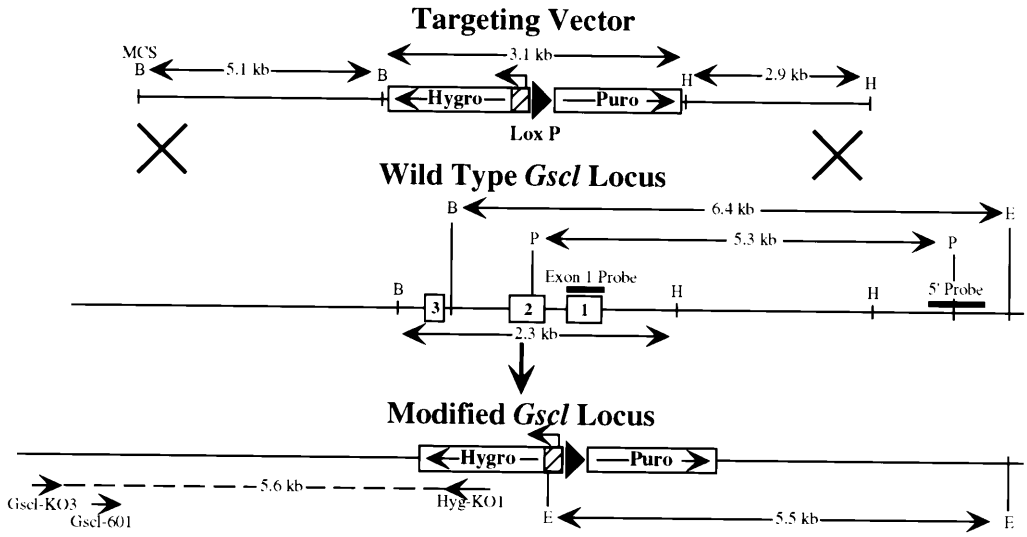

Figure 1. Strategy for targeted disruption of the *Gscl* gene by homologous recombination in mouse ES cells. The *Gscl* targeting vector (top) was constructed by inserting a 5.1 kb *Bam*HI fragment and a 2.9 kb *Hin*dIII fragment into pBluescript SK(+) (Stratagene). A 3.1 kb cassette containing a hygromycin resistance gene (Hygro) (56), a LoxP site (LoxP) and a promoterless puromycin resistance gene (Puro) (57) was inserted by blunt-end ligation into a *Sma*I site. A homologous recombination event (**XX**) between the targeting vector and the endogenous *Gscl* locus (middle) produced a modified *Gscl* locus (bottom). B, E, H and P denote the restriction sites *Bam*HI, *Eco*RI, *Hin*dIII and *Pvu*II, respectively; MCS corresponds to the Charon 35 phage multicloning site.

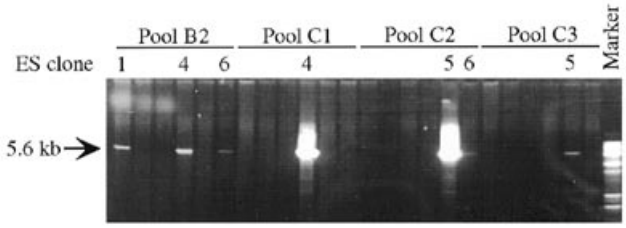

Figure 2. Identification of ES cell clones containing a modified *Gscl* locus by long-range PCR. Correctly targeted ES cell clones were identified by the presence of a 5.6 kb PCR product amplified using oligonucleotide primers Hyg-KO1 and Gscl-KO3 (Fig. 1). The specificity of the PCR products was confirmed by Southern blot hybridization with oligonucleotide Gscl-601 (Fig. 1). The lane labeled Marker contained a sample of λ phage DNA cut with *Bst*EII.

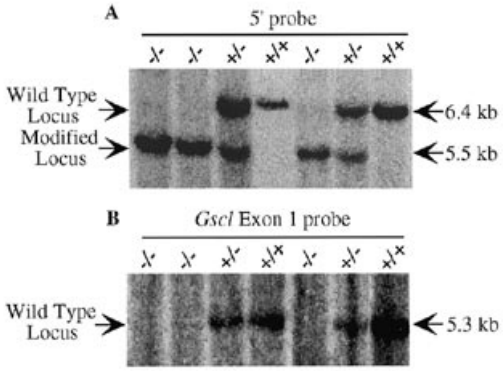

Figure 3. Genotype analysis of offspring from parents heterozygous for the modified *Gscl* allele. (**A**) Siblings that were heterozygous for the modified *Gscl* allele were bred and 10 µg tail DNA from offspring were digested with both *Eco*RI and *Bam*HI, blotted and hybridized with the 5′ probe (shown in Fig. 1, middle panel). (**B**) The same DNAs were digested with *Pvu*II, blotted and hybridized with *Gscl* exon 1 (Fig. 1). The deduced genotype of each animal is indicated above each lane.

portions of the 5′ and 3′ regions and since the Southern blotting experiments showed that no rearrangements had occurred that resulted in an intact *Gscl* gene, *Gscl* transcripts are expected to be completely absent in mice homozygous for the modified allele. *Gscl* transcripts are detectable during embryogenesis and in the testis of adult mice (30) as well as in newborn and adult mouse brain (Fig. 4). Total RNA from testes and brains of *Gscl* +/+, +/– and –/– animals was assayed for *Gscl* transcripts by RT–PCR using primers lying in exons 2 and 3. The expected 122 bp product was produced from the RNA of *Gscl* +/+ and +/– mice, but it was completely absent in reactions containing cDNA from *Gscl* –/– animals (Fig. 4). Generation of the 122 bp product in samples from animals containing at least one wild-type allele was completely dependent on the presence of reverse transcriptase (Fig. 4). As an internal control for production of cDNA by oligo(dT) priming and reverse transcription, all cDNA preparations were subjected to PCR with primers specific for the ubiquitously expressed *Sez12* gene. The expected 550 bp product was generated in all samples. We conclude that the modification introduced into the *Gscl* gene by homologous recombination indeed resulted in a null mutation.

Expression pattern of *Gscl* in mouse embryos

We reported previously that *Gscl* transcripts were detectable by RT–PCR in mouse embryos from E8.5 to 13.5 (30). The absence of such transcripts in northern blot analyses suggested very low level expression or possibly a highly localized expression pattern. To investigate the sites of *Gscl* expression during embryogenesis we carried out RNA *in situ* hybridization experiments to serial transverse and sagittal sections of mouse embryos from E8.5 to

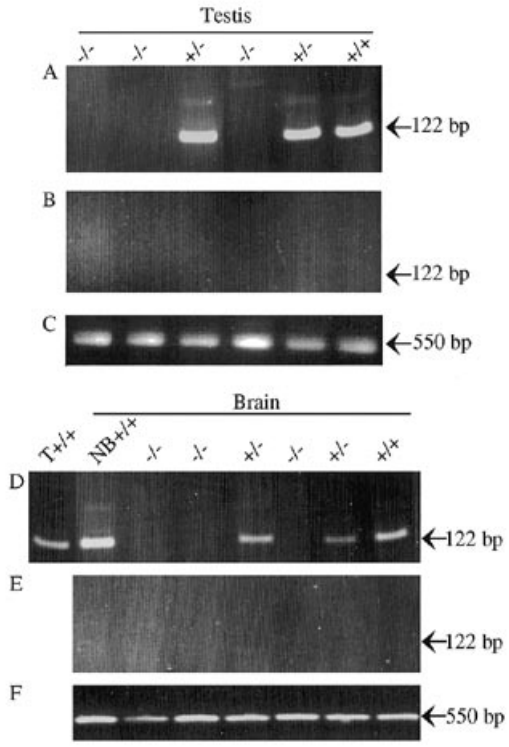

Figure 4. Analysis of *Gscl* mRNA levels in wild-type, heterozygous and homozygous *Gscl* mutant mice. Samples (0.5 µg) of total RNA isolated from testis and brain of 6- to 8-week-old littermates were subjected to RT–PCR with oligonucleotide primers Gscl-R and Gscl-3, which are specific for exon 2 and exon 3, respectively. The arrows in (A), (B), (D) and (E) indicate the positions of the expected 122 bp RT–PCR product. The genotype of each animal is indicated above each lane. Reactions carried out in the absence of any RNA (water) are shown, as is the migration of a 1 kb DNA ladder size marker. (**A–C**) Reactions with testis RNA samples. Reactions in (B) were performed in the absence of reverse transcriptase. Reactions in (C) were performed with primers specific for the mouse *IDD* (*Sez12*) gene as described previously (30). (**D–F**) Reactions with brain RNA samples. T +/+, testis RNA from a *Gscl* +/+ animal; NB +/+, newborn brain RNA from a *Gscl* +/+ animal. Reactions in (E) and (F) were performed as described for (B) and (C), respectively.

E12.5. Experiments were performed using antisense and sense probes corresponding to exon 3 and 460 bp of the putative 3′-untranslated region of *Gscl*. At E8.5, *Gscl* transcripts were detected in the endoderm of the ventral face of the rostral region of the foregut (Fig. 5B and C). Here *Gscl* expression is present in a region close to the first pharyngeal arch artery (Fig. 5B). By E11.5 *Gscl*-expressing cells become detectable at three sites in the developing brain. Relatively high expression was observed in the developing pons in a region containing the raphe nuclei, a system of serotonergic neurons (Fig. 6B). At this stage, *Gscl* expression was also detected in the choroid plexus of the fourth ventricle (Fig. 6C) as well as in the dorsal part of the neuroepithelium of the third ventricle, in a very specific region localized dorsal of the habenula (Fig. 6D). These sites of *Gscl* expression were also seen at E12.5 (data not shown). Because many of the abnormalities present in VCFS/DGS patients are thought to be due to a defect occurring in the pharyngeal arches, we examined these structures at various stages for *Gscl* expression. However, we failed to detect Gscl transcripts at any time in these regions.

Characterization of Gscl-deficient mice

Although the highly localized expression pattern of *Gscl* in embryos suggested that the gene may contribute to only a limited number of developmental processes, the *in situ* hybridization experiments cannot exclude low level expression at other sites. Therefore it was important to examine Gscl-deficient mice for any abnormal features. *Gscl* –/– mice exhibited normal birth weight and size and were indistinguishable from heterozygous and wild-type littermates. On necropsy, the sizes and weights of *Gscl* –/– mice were found to be within the normal range. To further characterize *Gscl* –/– mice, hematoxylin/eosin stained paraffin-embedded sections from 33 different tissues (see Materials and Methods) of 3-month-old mutant and control littermates were examined for pathological or abnormal histological features. No consistent differences between wild-type and homozygous mutant mice were detected. Since conotruncal heart defects are present in a high proportion of VCFS/DGS patients, special attention was given to analysis of the

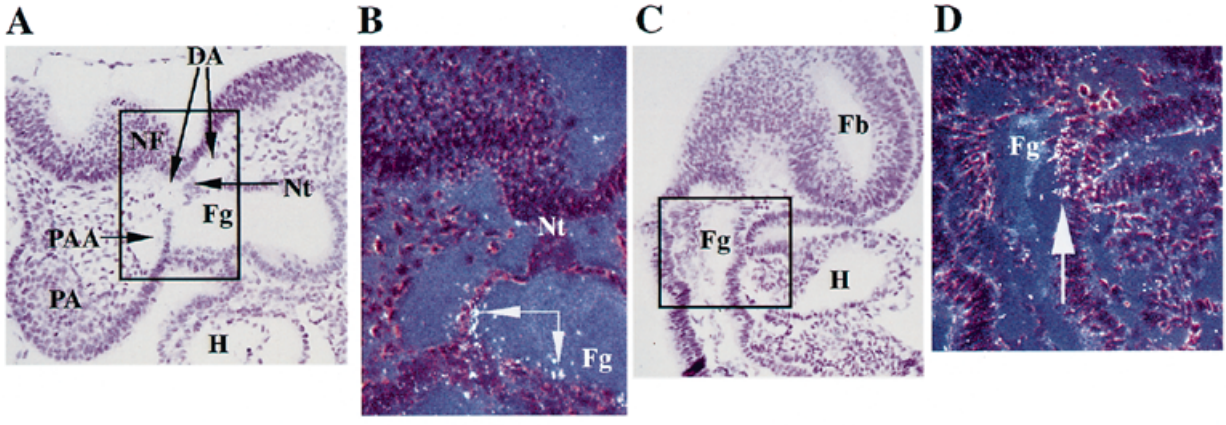

Figure 5. RNA *in situ* hybridization to *Gscl* transcripts in sections of E8.5 mouse embryos. (**A**) Transverse section of an E8.5 mouse embryo photographed in bright field (×20). (**B**) Boxed section enlarged from (A) showing detail of the foregut region (×40) photographed in dark field. Arrows indicate the positions of hybridization of *Gscl* transcripts (white dots in the dark field) in the endoderm of the foregut. (**C**) Sagittal section of an E8.5 mouse embryo photographed in bright field (×20). (**D**) Boxed section enlarged from (C) showing detail of the rostral part of the foregut region (×40) photographed in dark field. Arrow indicates the position of *Gscl* expression in the endoderm of the foregut. Hybridization with a sense *Gscl* probe to sections adjacent to those shown in (B) and (D) produced only background levels of autoradiographic signals. DA, dorsal aorta; Fb, forebrain; Fg, foregut; H, heart; NF, neural folds; Nt, notochord; PA, first pharyngeal arch; PAA, first pharyngeal arch artery.

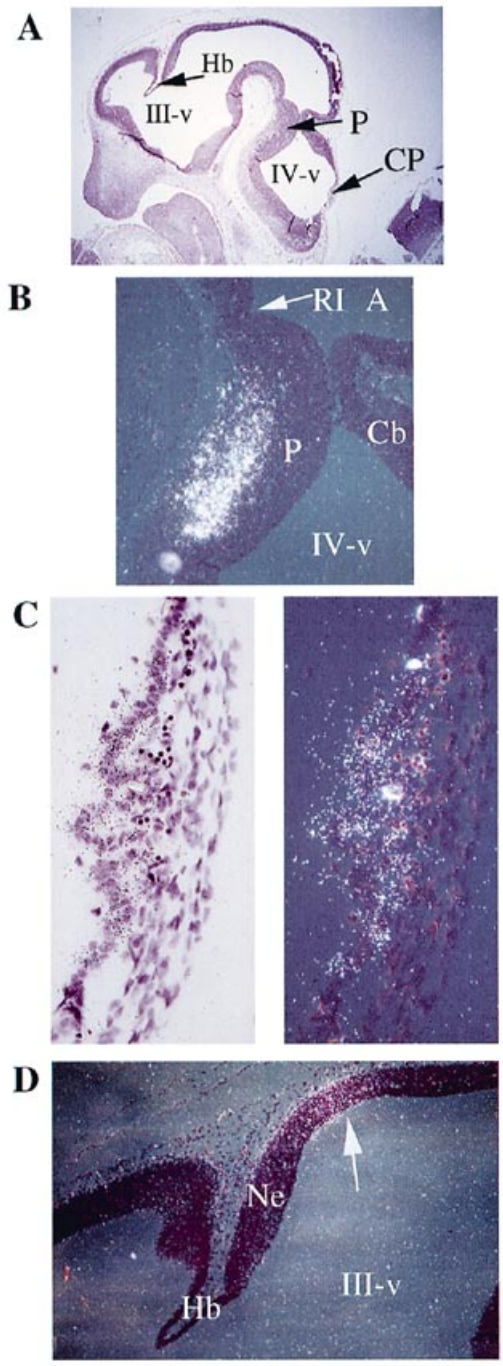

Figure 6. RNA *in situ* hybridization to *Gscl* transcripts in sections of E11.5 mouse embryos. (**A**) Sagittal section of the head of an E11.5 mouse embryo photographed in bright field (×2.5). (**B**) Enlargement of the pons region (×20) of the section shown in (A) photographed in dark field. (**C**) Enlargement of the choroid plexus from the fourth ventricle (×40), photographed in bright field (left) and in dark field (right). (**D**) Enlargement of the habenula and the dorsal part of the third ventricle (×10) photographed in dark field. Arrowhead indicates the position of *Gscl* expression in the dorsal part of the third ventricle. Hybridization with a sense *Gscl* probe to sections adjacent to those shown in (B), (C) and (D) produced only background levels of autoradiographic signals. III-v, third ventricle; IV-v, fourth ventricle; A, aqueduct of Sylvius; Cb, cerebellum; Hb, habenula; Ne, neuroepithelium; P, pons; RI, rhombic isthmus.

heart and the outflow tract. No abnormalities were detected either after examination of the heart and the conotruncal region during necropsy or when looking at the histological sections of the conotruncal region. These results indicate that the presence of the modified *Gscl* gene did not apparently impair normal development of the systems examined.

The RNA *in situ* hybridization experiments indicated highly localized expression of *Gscl* at several sites in the developing mouse brain. Therefore a detailed histological analysis of the central nervous system was performed on 1.5- to 3-month-old *Gscl* –/– mice and control littermates. The brain, spinal cord and optic chiasm were removed and coronal slices taken from the frontal, parietal and occipital levels of the cerebral hemispheres, from the cerebellum at the superior cerebellar peduncles and immediately caudal to the peduncles and from the spinal cord at the cervical, thoracic and lumbar levels. Ten micrometer paraffin-embedded sections were stained with hematoxylin/eosin for general cytoarchitecture, Luxol fast blue for myelin and by the Bodian technique for axons and examined by light microscopy (38). No consistent abnormalities were detected.

We reported previously that *Gscl* transcripts are detectable in adult mouse testis by RT–PCR (30) and a recent report indicates that *Gscl* is expressed in developing germ cells in embryonic gonadal tissue (39). Therefore, we examined testis development and spermatogenesis in adult *Gscl* –/– mice. Both the testis weights and the appearance of hematoxylin/eosin stained paraffin-embedded sections of the testes of *Gscl* –/– males were normal. *Gscl* –/– male and female animals were interbred. These matings produced litters of normal size and the progeny appeared normal. However, male rodents can produce normal sized litters even if they have a reduced number of mature sperm (40). Therefore, we also determined the number of epididymal sperm. Three 9-week-old *Gscl* –/– and wild-type male littermates were compared. The mature sperm number per animal was not different between homozygous mutants ($2.5 \pm 1.4 \times 10^7$) and wild-type ($2.6 \pm 1.2 \times 10^7$) males. These results indicate that the presence of the modified *Gscl* gene did not impair reproductive capacity nor production of mature sperm.

DISCUSSION

This report represents an attempt to investigate the etiology of an important multi-anomaly syndrome by inactivating the mouse ortholog of one of the genes in the VCFS/DGS commonly deleted region in chromosome 22q11. *Gscl* has been considered an excellent candidate for contributing to the developmental anomalies present in VCFS/DGS patients for several reasons. *GSCL* transcripts can be detected in 9- to 10-week human fetal tissue samples (30). More extensive analysis at various stages of embryogenesis in mice showed that the gene is expressed both during early development and at later times during organogenesis (30,41). Events that occur during both periods are relevant to the specific defects seen in VCFS/DGS patients. Furthermore, *Gscl* is highly related in its homeodomain to *Gsc* (30,36), which gene inactivation experiments have shown is required for proper craniofacial development (27,28,35). Despite this considerable circumstantial evidence pointing to a role for *Gscl* in VCFS/DGS etiology, the experiments reported here indicate that the gene is unlikely to be solely responsible for the developmental field defect thought to cause many of the anomalies seen in the patients. *Gscl* null mice are viable, they grow normally and are

fertile and they exhibit no detectable anatomical or histological abnormalities. The analysis included examination of 33 different tissues from 30-month-old *Gscl* –/– animals for pathological or abnormal histological features, as well as extensive histology of the central nervous system using three types of stains. Although no abnormalities were found in these mice, as discussed below, it is still quite possible that *Gscl* plays a role in one or more aspects of the syndromes.

Most VCFS/DGS patients have similar, large hemizygous deletions encompassing numerous genes. Although attempts to define a critical region through analysis of unique patients with other deletions or chromosomal rearrangements have not led to a consensus, all of the regions proposed contain multiple genes. Many of these genes have been isolated but to date there is no definitive evidence implicating any one of them in the etiology of the syndrome. The fact that such a large proportion of patients have extensive deletions could suggest that haploinsufficiency of more than one gene from the 22q11 region is responsible for development of the VCFS/DGS phenotype. There is ample precedent for dosage-sensitive genetic interactions between developmental control genes, including observations of functional synergism between a close relative of *Gscl*, *Goosecoid* (*Gsc*), and other genes. For example, compound mutants between *Gsc* and *Hepatic Nuclear Factor-3*β (*HNF3*β) of the genotype *Gsc* –/–; *Hnf3*B +/– exhibit developmental defects not seen in single gene mutants, either *Gsc* –/– or *Hnf3*β +/– mice (42). These defects occur in regions of the embryo where the two genes are co-expressed. Similarly, whereas *Gsc* –/– mice are born with normal limbs, *Gsc*/*Mhox* double mutant mice exhibit severe limb abnormalities (42,43). Thus, despite the absence of detectable abnormalities in *Gscl* –/– mice, *GSCL* still might play a role, in combination with hemizygosity of other genes in 22q11, in the developmental defects seen in VCFS/DGS patients. Our observation that *Gscl* is expressed in the rostral region of the developing foregut at E8.5 is particularly interesting, as this region gives rise to the embryonic pharynx and in turn portions of the adult nasal and oral cavities and larynx. Additional RNA *in situ* hybridization experiments are needed to evaluate the fate of Gscl-expressing cells in the foregut region of the embryo. Nevertheless, the observed expression of Gscl in this region of the foregut could suggest that hemizygosity of *Gscl*, along with another gene in 22q11, is involved in the velopharyngeal insufficiency seen frequently in VCFS/DGS patients. As mice bearing inactivating mutations in other genes from the VCFS/DGS region become available it will be possible to investigate combinatorial contributions of *Gscl* and the other genes to the VCFS/DGS phenotype by generating double mutant mice. Genes of particular interest in this context may be *Hira* and *Tbx1*, both of which, like *Gscl*, are expressed during embryogenesis and are presumptive nuclear proteins that affect transcriptional processes (44–46).

In addition to the possibility that hemizygosity of *Gscl* along with another gene(s) contributes to the developmental defect in VCFS/DGS, it is also possible that *Gscl* deficiency, either alone or in combination with another deficiency, is responsible for the learning disabilities and/or behavioral anomalies seen frequently in VCFS/DGS patients. In recent years it has become apparent that these patients frequently have psychiatric illnesses. The most common psychiatric diagnoses in adult patients are schizophrenia, schizoaffective disorder and bipolar spectrum disorders. Adolescent patients exhibit attention deficit disorder as well as mood disorders. RNA *in situ* hybridization experiments showed that *Gscl* transcripts are present in a highly localized pattern in three regions of the developing mouse brain at E11.5 and 12.5. Consistent with recently reported work by other investigators (39,47), we found *Gscl* transcripts in a subregion of the developing pons. In addition, we found expression of *Gscl* RNA at these times in the choroid plexus of the fourth ventricle as well as in the neuroepithelium of the third ventricle dorsal of the habenula, which defines the boundary of the forebrain and midbrain regions. It is difficult to speculate at this time about the significance of these observations for the learning disabilities and behavioral problems present in the patients. The highly specific pattern of expression in the developing pons may be most significant, as this region contains the raphe nuclei, serotonin-containing neurons that have been implicated in control of behavior. It should also be noted that we detected expression of *Gscl* in newborn and adult mouse brain RNA by RT–PCR (Fig. 4). *In situ* hybridization to sections of these tissues should prove to be informative for future investigations of *Gscl* –/– mice. Despite these intriguing observations, the detailed histological analysis of the entire central nervous system of adult *Gscl* –/– mice failed to reveal any abnormalities. Perhaps, as suggested above, deficiencies in the expression of more than one gene are involved in the etiology of the behavioral abnormalities in VCFS/DGS patients. Interestingly, another gene of unknown function, called *ES2*, lying adjacent to *Gscl* in the commonly deleted region, is co-expressed with *Gscl* in the pons in E14.5 mouse embryos (47). Furthermore, it has been suggested that reduced levels of catechol *O*-methyltransferase (COMT), which is encoded by another gene in the commonly deleted region, may be involved in the mood disorders seen in VCFS/DGS patients (48). A variety of experimental paradigms are available for testing the learning capacities and behavioral responses of rodents, including tests that are thought to be relevant to some of the behavioral anomalies present in VCFS/DGS patients. The mice produced in this study should be useful for evaluating the possibility that *Gscl* is involved in these aspects of the VCFS/DGS phenotype.

Whether or not *Gscl* is involved in the etiology of VCFS/DGS, the mice and ES cells described here that contain a targeted insertion of a LoxP site at the *Gscl* locus should prove invaluable for ascertaining the role of other genes in the VCFS/DGS commonly deleted region in the syndromes. The strategy for accomplishing this goal is to incorporate LoxP sites at various locations proximal and distal of *Gscl*. Then, by bringing two LoxP sites together, either by animal breeding or by sequential ES cell transfections, it is possible to induce specific deletions encompassing different sets of genes by Cre-mediated recombination (49). The reagents generated during the course of the current work represent the first step towards such genetic manipulations.

MATERIALS AND METHODS

Disruption of the *Gscl* gene in ES cells and generation of chimeric mice

Clone WW6 ES cells were cultured according to Ioffe (37). *Not*I-linearized targeting vector (20 μg) was electroporated into 7×10^7 ES cells. ES cell colonies resistant to 150 μg/ml hygromycin (Boehringer Mannheim) were isolated and expanded. About 1 μg DNA prepared from pooled ES cells (6

colonies/pool) was analyzed using the Expand long template PCR kit (Boehringer Mannheim) using primers Gscl-KO3 (5′-ggggcagggtcagatacatgacga-3′) and Hyg-KO1 (5′-tactcgccgatagtggaaaccgac-3′) (Fig. 1). PCR amplification cycles were as follows: 92°C for 10 s, 65°C for 30 s, 68°C for 3 min for 10 cycles followed by 25 cycles using the same conditions with addition of 10 s to each elongation step. PCR products were electrophoresed in an agarose gel and transferred to a Hybond N membrane (Amersham). The specificity of the 5.6 kb PCR product (Fig. 2) was assessed by hybridization with 20 ng internal primer Gscl-601 (5′-atggatgagtggtggccaca-3′) (Fig. 1) that was radiolabeled by a 3′-kinase reaction (New England Biolabs) as described by Hazan *et al*. (50). ES cell clones were injected into C57BL/6 recipient blastocysts which were transferred to CD-1 pseudopregnant females (51). Two ES cell clones (A16 and 1A5) produced chimeras which were used for breeding and analysis. For mouse genotyping, PCR reactions were set up to screen for the wild-type allele and the modified allele using primers Gscl-E (5′-agctggttggtagtgcct-3′) and Gscl-F (5′-aggagagttgttgatgctg-3′) and primers Gscl-E and Hyg-KO1, respectively. For Southern blot hybridization (52), ES cell and mouse tail DNAs were prepared as described (53). The 5′ probe (Fig. 1) used to detect wild-type and recombinant alleles was generated by PCR using primers Gscl-KOA (5′-agcttccccagggattctg-3′) and Gscl-KOBr (5′-cagcagcaggtaggactgga-3′).

Reverse transcriptase-mediated polymerase chain reaction

Total mouse tissue RNA was isolated using Trizol reagent (Gibco) following the manufacturer's instructions and northern blot hybridization was performed as described (52). After DNase RQ1 (Promega) treatment, 5 µg of total RNA were reverse transcribed with oligo(dT) primers using the SuperScript II kit (Gibco BRL) following the manufacturer's instructions. PCR was performed on one tenth volume of the reverse transcription reaction using primers Gscl-R (5′-gagaggagcgcgtggag-3′) and Gscl-3 (5′-gcatcaacaactctccttgg-3′) with an annealing temperature of 56°C. The specificity of the 122 bp product was checked by hybridization with primer Gscl-T (5′-cttttggtgtcgccactttgcc-3′) as described above. The cDNA integrity was checked by PCR amplification with primer specific for the ubiquitously expressed *Sez12* gene as described (30).

Histological analysis of mouse tissues

For analysis of central nervous system tissues, mice were anesthetized and perfused via the left cardiac ventricle with 20 ml cold phosphate-buffered 4% paraformaldehyde. The brain, spinal cord and optic chiasm were removed, coronal slices were taken from the frontal, parietal and occipital levels of the cerebral hemispheres, from the cerebellum at the superior cerebellar peduncles and immediately caudal to the peduncles and from the spinal cord at the cervical, thoracic and lumbar levels. The tissue was dehydrated and embedded in paraffin. Ten micrometer sections were stained with hematoxylin and eosin for general cytoarchitecture, Luxol fast blue for myelin and by the Bodian technique (38) for axons and examined by light microscopy. For histological analysis of other organs, tissues were dissected, fixed in neutral buffered 10% formalin and embedded in paraffin. Five micrometer sections were prepared and stained with hematoxylin and eosin. Two to three sections of each tissue were examined by light microscopy by Dr Linda Johnson, a veterinary pathologist in the Albert Einstein College of Medicine Animal Institute. The following tissues were examined: calvarium, eye, salivary glands, pharynx, trachea, esophagus, thyroid, parathyroid, thymus, pituitary, heart, diaphragm, lung, spleen, liver, kidney, adrenal, stomach, pancreas, intestine, colon, cervical, thoracic and lumbar vertebrae, tibia, femur, sternum, uterus, prostate, testis, epididymis, seminal vesicle, coagulating and prepucial glands and urinary bladder.

Sperm counting

Epididymes were removed from three 9-week-old homozygous and wild-type males under sterile conditions and placed in a dish containing 1 ml DMEM medium (Gibco) (54). The sperm were allowed to disperse into the medium for 2 h at room temperature and the number of spermatozoa was determined by counting in a hematocytometer.

RNA *in situ* hybridization

For RNA *in situ* hybridization a 570 bp probe (Gscl-3′) encompassing the third exon and a portion of the putative 3′-untranslated region was generated by PCR of genomic DNA using primers Gscl-3A (5′-cctcaggtctggttcaagaa-3′) and Gscl-X (5′-tggcatcagctcaaggct-3′). The PCR product was cloned into the PCR 2.1 plasmid from the TA Cloning Kit (Invitrogen) and then subcloned into pBluescript SK. Sense and antisense ^{33}P-labeled RNA probes were synthesized from linearized plasmid DNA, using either T3 or T7 RNA polymerase, respectively. Hybridization to paraffin-embedded embryo sections (Novagen) was performed according to a published protocol (55). Hybridization was carried out at 60°C for 16 h in 50% deionized formamide, 0.3 M NaCl, 20 mM Tris–HCl, pH 7.4, 5 mM EDTA, 10 mM Denhardt's solution, 500 µg/ml yeast RNA, 0.1 M DTT with 5×10^6 d.p.m./ml ^{33}P-labeled RNA probe. After hybridization, sections were washed sequentially as follows: (i) 5× SSC, 10 mM DTT at 50°C for 30 min; (ii) 50% formamide, 2× SSC, 0.1 M DTT at 65°C for 20 min; (iii) twice in 0.1 M Tris–HCl, pH 7.5, 0.4 M NaCl, 50 mM EDTA for 10 min at 37°C; (iv) once in the same solution as in step (iii) but with 20 µg/ml RNase A at 37°C for 15 min. The slides were then dehydrated rapidly and processed for standard autoradiography using Kodak NTB-2 emulsion and exposed for 2–4 weeks at 4°C. After developing in Kodak D-19 developer and fixer, the sections were stained with hematoxylin and eosin and mounted. Observations and photography were carried out using both bright and dark fields on a Zeiss Axiophot microscope.

ACKNOWLEDGEMENTS

We thank Hui Xu for excellent technical assistance, Karen Witty-Bleeps for her technical support for the RNA *in situ* hybridization experiments and Dr Ron DePinho and Harry Hou of the Albert Einstein College of Medicine Comprehensive Cancer Center Gene Targeting Facility for mouse blastocyst injections. We also thank Drs Zaven Kaprielian, Elizabeth Lacy, Katia Manova, Bernice Morrow and David Weinstein for helpful discussions. Dr Howard Sirotkin kindly provided the hygromycin–LoxP–puromycin cassette used to construct the targeting vector. This work was supported by NIH grant HD34890.

ABBREVIATIONS

DGS, DiGeorge syndrome; ES cell, embryonic stem cell; Gsc, goosecoid; Gscl, goosecoid-like; Hnf3β, hepatic nuclear factor-3β; VCFS, velocardiofacial syndrome.

REFERENCES

1. Driscoll,D.A., Budarf,M.L. and Emanuel,B.S. (1992) A genetic etiology for DiGeorge syndrome: consistent deletions and microdeletions of 22q11. *Am. J. Hum. Genet.*, **50**, 924–933.
2. Driscoll,D.A., Spinner,N.B., Budarf,M.L., McDonald-McGinn,D.M., Zackai,E.H., Goldberg,R.B., Shprintzen,R.J., Saal,H.M., Zonana,J., Jones,M.C. and Emanuel,B.S. (1992) Deletions and microdeletions of 22q11.2 in velo-cardio-facial syndrome. *Am. J. Med. Genet.*, **44**, 261–268.
3. Burn,J. and Goodship,J. (1996) In Rimoin,D.L., Connor,J.M. and Pyeritz,R.E. (eds), *Embery and Rimoin's Principles and Practice of Medical Genetics*. Churchill Livingstone, New York, NY, pp. 767–828.
4. Goldberg,R., Motzkin,B., Marion,R., Scambler,P.J. and Shprintzen,R.J. (1993) Velo-cardio-facial syndrome: a review of 120 patients. *Am. J. Med. Genet.*, **45**, 313–319.
5. Thomas,J.A. and Graham,J.,Jr (1997) Chromosomes 22q11 deletion syndrome: an update and review for the primary pediatrician. *Clin. Pediat.*, **36**, 253–266.
6. Motzkin,B., Marion,R., Goldberg,R., Shprintzen,R. and Saenger,P. (1993) Variable phenotypes in Velo-cardio-facial syndrome with chromosomal deletion. *J. Pediat.*, **123**, 406–410.
7. Papolos,D.F., Faedda,G.L., Veit,S., Goldberg,R., Morrow,B., Kucherlapati,R. and Shprintzen,R.J. (1996) Bipolar spectrum disorders in patients diagnosed with Velo-cardio-facial syndrome: does a hemizygous deletion of chromosome 22q11 result in bipolar affective disorder? *Am. J. Psychiat.*, **153**, 1541–1547.
8. Carlson,C., Papolos,D., Pandita,R.K., Faedda,G.L., Veit,S., Goldberg,R., Shprintzen,R., Kucherlapati,R. and Morrow,B. (1997) Molecular analysis of velo-cardio-facial syndrome patients with psychiatric disorders. *Am. J. Hum. Genet.*, **60**, 851–859.
9. Driscoll,D.A., Salvin,J., Sellinger,B., Budarf,M.L., McDonald-McGinn,D.M., Zackai,E.H. and Emanuel,B.S. (1993) Prevalence of 22q11 microdeletions in DiGeorge and velocardiofacial syndromes: implications for genetic counseling and prenatal diagnosis. *J. Med. Genet.*, **30**, 813–817.
10. Lindsay,E.A., Goldberg,R., Jurecic,V., Morrow,B., Carlson,C., Kucherlapati,R.S., Shprintzen,R.J. and Baldini,A. (1995) Velo-cardio-facial syndrome: frequency and extent of 22q11 deletions. *Am. J. Med. Genet.*, **57**, 514–522.
11. Morrow,B., Goldberg,R., Carlson,C., Das Gupta,R., Sirotkin,H., Collins,J., Dunham,I., O'Donnell,H., Scambler,P., Shprintzen,R. and Kucherlapati,R. (1995) Molecular definition of the 22q11 deletions in Velo-cardio-facial syndrome. *Am. J. Hum. Genet.*, **56**, 1391–1403.
12. Carlson,C., Sirotkin,H., Pandita,R., Goldberg,R., McKie,J., Wadey,R., Patanjali,S.R., Weissman,S.M., Anyane-Yeboa,K., Warburton,D., Scambler,P., Shprintzen,R., Kucherlapati,R. and Morrow,B.E. (1997) Molecular definition of 22q11 deletions in 151 velo-cardio-facial syndrome patients. *Am. J. Hum. Genet.*, **61**, 620–629.
13. Dallapiccola,B., Pizzuti,A. and Novelli,G. (1996) How many breaks do we need to CATCH on 22q11?. *Am. J. Hum. Genet.*, **59**, 7–11.
14. Budarf,M.L. and Emanuel,B.S. (1997) Progress in the autosomal segmental aneusomy syndromes (SASs): single or multi-locus disorders? *Hum. Mol. Genet.*, **6**, 1657–1665.
15. Brown,J., Dry,K.L., Edgar,A.J., Pryde,F.E., Hardwick,L.J., Aldred,M.A., Lester,D.H., Boyle,S., Kaplan,J., Dufier,J.L., Ho,M.F., Monaco,A.M., Musarella,M.A. and Wright,A.F. (1996) Analysis of three deletion breakpoints in Xp21.1 and the further localization of RP3. *Genomics*, **37**, 200–210.
16. Crolla,J.A., Cross,I., Atkey,N., Wright,M. and Oley,C.A. (1996) FISH studies in a patient with sporadic aniridia and t(7;11) (q31.2;p13). *J. Med. Genet.*, **33**, 66–68.
17. Wirth,J., Wagner,T., Meyer,J., Pfeiffer,R.A., Tietze,H.U., Schempp,W. and Scherer,G. (1996) Translocation breakpoints in three patients with Campomelic Dysphasia and autosomal sex reversal map more than 130 kb from SOX9. *Hum. Genet.*, **97**, 186–193.
18. Sutherland,H.F., Wadey,R., McKie,J.M., Taylor,C., Atif,U., Johnstone,K.A., Halford,S., Kim,U.J., Goodship,J., Baldini,A. and Scambler,P.J. (1996) Identification of a novel transcript disrupted by a balanced translocation associated with DiGeorge syndrome. *Am. J. Hum. Genet.*, **59**, 23–31.
19. Le Douarin,N. (1980) *The Neural Crest*. Cambridge University Press, Cambridge, UK.
20. Le Douarin,N.M., Ziller,C. and Couly,G.F. (1993) Patterning of neural crest derivatives in the avian embryo: *in vivo* and *in vitro* studies. *Dev. Biol.*, **159**, 24–49.
21. Kirby,M.L. and Waldo,K.L. (1995) Neural crest and cardiovascular patterning. *Circulation Res.*, **77**, 211–215.
22. Mark,M., Rijli,F.M. and Chambon,P. (1997) Homeobox genes in embryogenesis and pathogenesis. *Pediat. Res.*, **42**, 421–429.
23. Boncinelli,E. (1997) Homeobox genes and disease. *Curr. Opin. Genet. Dev.*, **7**, 331–337.
24. Innis,J.W. (1997) Role of HOX genes in human development. *Curr. Opin. Pediat.*, **9**, 617–622.
25. Schilling,T.F. (1997) Genetic analysis of craniofacial development in the vertebrate embryo. *Bioessays*, **19**, 459–468.
26. Chisaka,O. and Capecchi,M.R. (1991) Regionally restricted developmental defects resulting from targeted disruption of the mouse homeobox gene hox-1.5. *Nature*, **350**, 473–479.
27. Rivera-Perez,J.A., Mallo,M., Gendron-Maguire,M., Gridley,T. and Behringer,R.R. (1995) Goosecoid is not an essential component of the mouse gastrula organizer but is required for craniofacial and rib development. *Development*, **121**, 3005–3012.
28. Yamada,G., Mansouri,A., Torres,M., Stuart,E.T., Blum,M., Schultz,M., De Robertis,E.M. and Gruss,P. (1995) Targeted mutation of the murine goosecoid gene results in craniofacial defects and neonatal death. *Development*, **121**, 2917–2922.
29. Conway,S.J., Henderson,D.J. and Copp,A.J. (1997) Pax3 is required for cardiac neural crest migration in the mouse: evidence from the splotch (Sp2H) mutant. *Development*, **124**, 505–514.
30. Funke,B., Saint-Jore,B., Puech,A., Sirotkin,H., Edelmann,L., Carlson,C., Raft,S., Pandita,R.K., Kucherlapati,R., Skoultchi,A. and Morrow,B.E. (1997) Characterization and mutation analysis of goosecoid-like (GSCL), a homeodomain-containing gene that maps to the critical region for VCFS/DGS on 22q11. *Genomics*, **46**, 364–372.
31. Gottlieb,S., Emanuel,B.S., Driscoll,D.A., Sellinger,B., Wang,Z., Roe,B. and Budarf,M.L. (1997) The DiGeorge syndrome minimal critical region contains a goosecoid-like (GSCL) homeobox gene that is expressed early in human development. *Am. J. Hum. Genet.*, **60**, 1194–1201.
32. Blum,M., De Robertis,E.M., Kojis,T., Heinzmann,C., Klisak,I., Geissert,D. and Sparkes,R.S. (1994) Molecular cloning of the human homeobox gene goosecoid (GSC) and mapping of the gene to human chromosome 14q32.1. *Genomics*, **21**, 388–393.
33. Blum,M., Gaunt,S.J., Cho,K.W., Steinbeisser,H., Blumberg,B., Bittner,D. and De Robertis,E.M. (1992) Gastrulation in the mouse: the role of the homeobox gene goosecoid. *Cell*, **69**, 1097–1106.
34. Gaunt,S.J., Blum,M. and De Robertis,E.M. (1993) Expression of the mouse goosecoid gene during mid-embryogenesis may mark mesenchymal cell lineages in the developing head, limbs and body wall. *Development*, **117**, 769–778.
35. Zhu,C.C., Yamada,G. and Blum,M. (1997) Correlation between loss of middle ear bones and altered goosecoid gene expression in the branchial region following retinoic acid treatment of mouse embryos *in vivo*. *Biochem. Biophys. Res. Commun.*, **235**, 748–753.
36. Galili,N., Baldwin,H.S., Lund,J., Reeves,R., Gong,W., Wang,Z., Roe,B.A., Emanuel,B.S., Nayak,S., Mickanin,C., Budarf,M.I. and Buck,C.A. (1997) A region of mouse chromosome 16 is syntenic to the DiGeorge, velo-cardio-facial syndrome minimal critical region. *Genome Res.*, **7**, 17–26.
37. Ioffe,E., Liu,Y., Bhaumik,M., Poirier,F., Factor,S. and Stanley,P. (1995) WW6: an embryonic stem cell line with an inert genetic marker that can be traced in chimeras. *Proc. Natl Acad. Sci. USA*, **92**, 7357–7361.
38. Davis,R.L. and Robertson,D.M. (1997) *Textbook of Neuropathology*. Williams & Wilkins, Baltimore, MD.
39. Galili,N., Epstein,J.A., Leconte,I., Nayak,S. and Buck,C.A. (1998) Gscl, a gene within the minimal DiGeorge critical region, is expressed in primordial germ cells and the developing pons. *Dev. Dyn.*, **212**, 86–93.
40. Ratnasooriya,W.D. and Sharpe,R.M. (1989) Evaluation of the effect of selective germ cell depletion on subsequent spermatogenesis and fertility in the rat. *Int. J. Androl.*, **12**, 44–57.
41. Wakamiya,M., Riviera-Perez,J.A., Baldini,A. and Behringer,R.R. (1997) Goosecoid and Goosecoid-related genes in mouse embryogenesis. *Cold Spring Harbor Symp. Quant. Biol.*, **62**, 145–149.

42. Filosa,S., Rivera-Perez,J.A., Gomez,A.P., Gansmuller,A., Sasaki,H., Behringer,R.R. and Ang,S.L. (1997) Goosecoid and HNF-3β genetically interact to regulate neural tube patterning during mouse embryogenesis. *Development*, **124**, 2843–2854.
43. Martin,J.F., Bradley,A. and Olson,E.N. (1995) The paired-like homeo box gene *MHox* is required for early events of skeletogenesis in multiple lineages. *Genes Dev.*, **9**, 1237–1249.
44. Wilming,L.G., Snoeren,C.A., van Rijswijk,A., Grosveld,F. and Meijers,C. (1997) The murine homologue of HIRA, a DiGeorge syndrome candidate gene, is expressed in embryonic structures affected in human CATCH22 patients. *Hum. Mol. Genet.*, **6**, 247–258.
45. Chapman,D.L., Garvey,N., Hancock,S., Alexiou,M., Agulnik,S.I., Gibson-Brown,J.J., Cebra-Thomas,J., Bollag,R.J., Silver,L.M. and Papaioannou,V.E. (1996) Expression of the T-box family genes, Tbx1–Tbx5, during early mouse development. *Dev. Dyn.*, **206**, 379–390.
46. Chieffo,C., Garvey,N., Gong,W., Roe,B., Zhang,G., Silver,L., Emanuel,B.S. and Budarf,M.L. (1997) Isolation and characterization of a gene from the DiGeorge chromosomal region homologous to the mouse Tbx1 gene. *Genomics*, **43**, 267–277.
47. Lindsay,E.A., Harvey,E.L., Scambler,P.J. and Baldini,A. (1998) ES2, a gene deleted in DiGeorge syndrome, encodes a nuclear protein and is expressed during early mouse development, where it shares an expression domain with a Goosecoid-like gene. *Hum. Mol. Genet.*, **7**, 629–635.
48. Lachman,H.M., Morrow,B., Shprintzen,R., Veit,S., Parsia,S.S., Faedda,G., Goldberg,R., Kucherlapati,R. and Papolos,D.F. (1996) Association of codon 108/158 catechol-*O*-methyltransferase gene polymorphism with the psychiatric manifestations of velo-cardio-facial syndrome. *Am. J. Med. Genet.*, **67**, 468–472.
49. Ramirez-Solis,R., Liu,P. and Bradley,A. (1995) Chromosome engineering in mice. *Nature*, **378**, 720–724.
50. Hazan,J., Dubay,C., Pankowiak,M.P., Becuwe,N. and Weissenbach,J. (1992) A genetic linkage map of human chromosome 20 composed entirely of microsatellite markers. *Genomics*, **12**, 183–189.
51. Robertson,E.J. (1987) *Tetracarcinomas and Embryonic Stem Cells*. IRL press, Oxford, UK.
52. Sambrook,J., Fritsch,E.F. and Maniatis,T. (1989) *Molecular Cloning: A Laboratory Manual*. Cold Spring Harbor Laboratory Press, Cold Spring Harbor, NY.
53. Laird,P.W., Zijderveld,A., Linders,K., Rudnicki,M.A., Jaenisch,R. and Berns,A. (1991) Simplified mammalian DNA isolation procedure. *Nucleic Acids Res.*, **19**, 4293.
54. Cohen,P.E., Chisholm,O., Arceci,R.J., Stanley,E.R. and Pollard,J.W. (1996). Absence of colony-stimulating factor-1 in osteopetrotic ($csfm^{op}/csfm^{op}$) mice results in male fertility defects. *Biol. Reprod.*, **55**, 310–317.
55. Wilkinson,D. (1992) *In Situ Hybridization: A Practical Approach*. IRL Press, Oxford, UK.
56. Bernard,H.U., Krammer,G. and Rowekamp,W.G. (1985) Construction of a fusion gene that confers resistance against hygromycin B to mammalian cells in culture. *Exp. Cell Res.*, **158**, 237–243.
57. de la Luna,S., Soria,I., Pulido,D., Ortin,J. and Jimenez,A. (1988) Efficient transformation of mammalian cells with constructs containing a puromycin-resistance marker. *Gene*, **62**, 121–126.